Zhenlei Liu*, Kang Yang and Dejun Yan

Refill Friction Stir Spot Welding of Dissimilar 6061/7075 Aluminum Alloy

https://doi.org/10.1515/htmp-2017-0139
Received October 11, 2017; accepted May 03, 2018

Abstract: Refill friction stir spot welding (RFSSW) was used to join 6061-T6 and 7075-T6 aluminum alloys in this work. Different sheet configurations and welding parameters were used to optimize joint strength. The effect of sleeve plunge depth on the microstructure and mechanical properties of the joints were investigated. The results showed that no defects were obtained when 6061-T6 aluminum alloy was placed as the upper sheet. The lap shear failure load of the joint using 6061-T6 aluminum alloy as the upper sheet was higher than that using 7075-T6 as the upper sheet. The maximum failure load of 12,892 N was attained when using the sleeve plunge depth of 3.6 mm. The joint failed at the upward flowing 7075 near the hook.

Keywords: refill friction stir spot welding, sheet configuration, microstructure, lap shear failure load

Introduction

In the twenty-first century, the global energy crisis causes light-weight materials to be extensively used in automobile industries [1, 2]. Aluminum alloys, which own low densities, high specific strengths and good corrosion resistance, are of great potential in industries. 7075 Al is one of the high-strength alloys and is always used as structural components such as aircraft fuselage panels and airplane wings [3]. 6061 Al is one of the middle-strength alloys and is always used on high-speed trains. It is of great significance to obtain 7075/6061 joint with satisfied mechanical properties.

As is well-known, it was always unsuccessful to join aluminum alloys using fusion welding technologies because defects such as cracks, porosities and high residual stresses easily appeared [4]. Friction stir welding (FSW) was invented in the 1990s to join aluminum alloys. During FSW, peak temperature is commonly lower than the melting points of base materials (BMs). Therefore, a plenty of the fusion defects can be avoided [5]. Till now, a lot of works have been done to investigate the microstructure and mechanical properties of FSW joints [4–12]. Yan et al. [4] butt welded dissimilar Al–Mg–Si/Al–Zn–Mg aluminum alloys using different configuration and reported that tensile strengths of the dissimilar Al–Mg–Si/Al–Zn–Mg joints using both configurations were higher than that of the Al–Mg–Si FSW joint. Guo et al. [12] reported that better material mixing was obtained when 6061 served as the advancing side. In recent years, FSW has been used to join some new materials such as Ti alloys [6–8], Cu alloys [9], steels [10] and even composite materials [11].

Refill friction stir spot welding (RFSSW) is a new variant of FSW, which was invented in 2002 by GKSS-GmbH [13]. The most significant feature of RFSSW was that it can eliminate the keyholes. RFSSW showed great potential among spot joining technologies and is now considered as a promising technology to replace riveting and resistance spot joining [14–28]. The tool used in RFSSW is more complicated, which consists of a clamping ring, whose main function is to keep the plates tightly and avoid plastic material from escaping, and a pin and a sleeve, which are the main components to stir the material. By adopting different movements to the three components, plastic material can be refilled back into joint after RFSSW and spot joint without keyhole can be obtained. Zhao et al. [14] studied the effect of plunge depth on microstructure and mechanical properties of 7B04 Al RFSSW joints and found that the position of bonding ligament gradually migrated downwards with increasing the plunge depth. Shen et al. [15] reported that the thermal-mechanically affected zone/stir zone (TMAZ/SZ) interface and the original lap interface were the weak regions for RFSSW joint. Similar conclusion was obtained by Li et al. [16] and the fracture mechanism of RFSSW joint was detailed discussed in that work. Suhuddin et al. [17, 18] reported that the intermetallic compounds of $Al_{12}Mg_{17}$ and Al_3Mg_2 formed in dissimilar Al/Mg joints and they significantly affected joint strength. Campanelli et al. [19] reported that high joint strength was obtained by increasing the material mixing and simultaneously minimizing the hook

***Corresponding author: Zhenlei Liu,** Faculty of Aerospace Engineering, Shenyang Aerospace University, Shenyang 110136, China, E-mail: hit_liuzhenlei@yeah.net
Kang Yang, Faculty of Aerospace Engineering, Shenyang Aerospace University, Shenyang 110136, China, E-mail: ykangok@163.com
Dejun Yan, Guangdong Key Laboratory of Enterprise Advanced Welding Technology for Ships, CSSC Huangpu Wenchong Shipbuilding Company Limited, Guangzhou 510715, China, E-mail: yandejun_2003@163.com

height. Cao et al. [27, 28] found that the hook in 6061 RFSSW joint was closely associated to sleeve plunge depth and higher hook resulted into lower joint strength.

In this work, RFSSW was used to join 6061/7075 aluminum alloys. The optimum joint strength was obtained by changing different welding parameters. The microstructure and mechanical properties of RFSSW joint were studied.

Experiment

Three mm-thick 6061-T6 and 7075-T6 aluminum alloys were chosen as the BM in this work. The sheets were cut into dimensions of 140 mm × 40 mm. Before welding, the surfaces of the sheets were polished using 500 # emery papers and cleaned in acetone. During welding, two sheets were lap combined using a width of 50 mm. The schematic of the joint is shown in Figure 1.

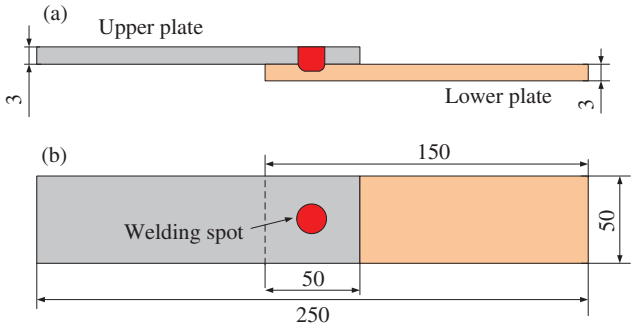

Figure 1: Schematic of the joint (unit mm).

The RFSSW machine used during experiment was RPS100SK10. The outer diameters of the clamping ring, sleeve and pin were 14.5 mm, 9 mm and 5 mm. The inner diameters of the clamping ring and the sleeve was 9.2 mm and 5.2 mm. The welding speed was chosen as 1600 rpm. Different sleeve plunge depths were 3.4 mm, 3.5 mm, 3.6 mm and 3.7 mm. The sleeve plunge and retract speeds were both 50 mm/min. After welding, metallographic samples were cut through joint centers and then were polished using standard polishing procedure. After etched using Keller's reagent for 20 s, the cross sections of joints were taken using an optical microscopy (OM VHX-1000E). The microstructure was then observed using a scanning electron microscope (SEM, SU3500 made by Hitachi, Japan). Room temperature lap shear tests were performed using a constant speed of 3 mm/min. The fracture positions were observed by OM.

Results and discussion

Joint cross section morphology

Figure 2 shows the microstructure of the joint using 7075 as the upper sheet. The sleeve plunge depth was 3.4 mm. The joint cross section presented a basin-like morphology. Defects such as un-bonded interface, voids and incomplete refilling were observed (Figure 2(a)). Un-bonded interface was observed at the joint center. This was attributed to relative weak material flow behavior at the joint center. Shen et al. [15] reported that the grain size at the pin affected zone was bigger than that at the sleeve affected zone. Besides, Li et al. [29] reported that void was observed at the joint center. Therefore, increasing the material flow behavior at the joint center was an effective method to avoid the un-bonded interface.

At the TMAZ/SZ interface near the maximum plunge depth, small voids were observed. For FSW butt joint, void is commonly considered as insufficient material flow behavior. In this work, the authors believed that the void was formed because of both material loss and the bad material flow-ability of 7075 alloy. During welding, a part of plastic material, which was extruded into the gap between the tool components, cannot be refilled back after welding. The material loss led to void. Besides, the heat input was not sufficient to soften the material to be a good plasticity, leading to voids.

At the TMAZ/SZ interface near joint upper surface, incomplete refilling was observed (Figure 2(d)). Incomplete refilling has been reported in the works of Shen et al. [15], Li et al. [30] and Xu et al. [31]. Shen et al. [15] attributed this defect to different slip conditions of the material at the TMAZ/SZ interface. Xu et al. [29] used a small plunge of the tool to eliminate this defect. Li et al. [16, 30] thought this defect was formed because of the weak diffusion bonding effect and residual stress.

Figure 3 shows the hook of the RFSSW joints using different sheet configurations. As shown in Figure 3(a), the interface presented an upward bending morphology on the joint using 6061 as upper sheet. There existed a partially bonded region and it has a width of about 110 μm. From the partially bonded region to the sleeve retraction path, a fully bonded region with a width of about 150 μm was observed. Figure 3(b) shows the hook of the joint using 7075 as the upper sheet. From the un-bonded lap interface to the SZ, the partially bonded region had a width of about 90 μm and the fully bonded region has a width of about 50 μm. When 6061 was placed as the upper sheet, better flowability of SZ was obtained compared with

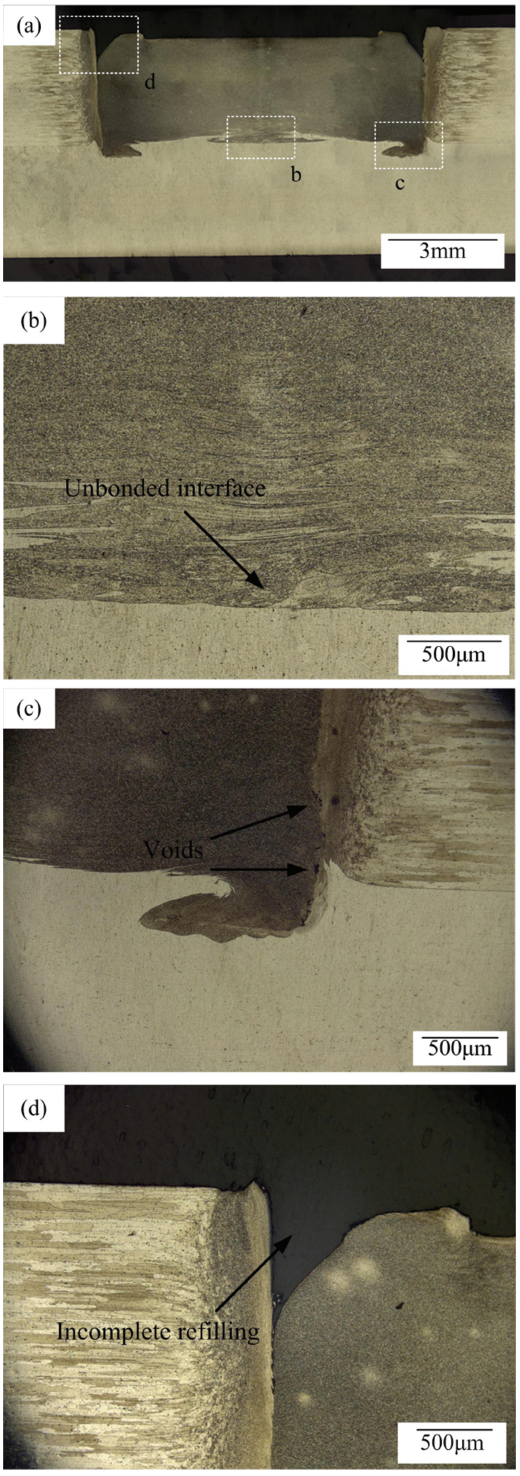

Figure 2: Microstructure of the joint using 7075 as the upper sheet (a) cross section, (b) un-bonded interface (c) void and (d) incomplete refilling.

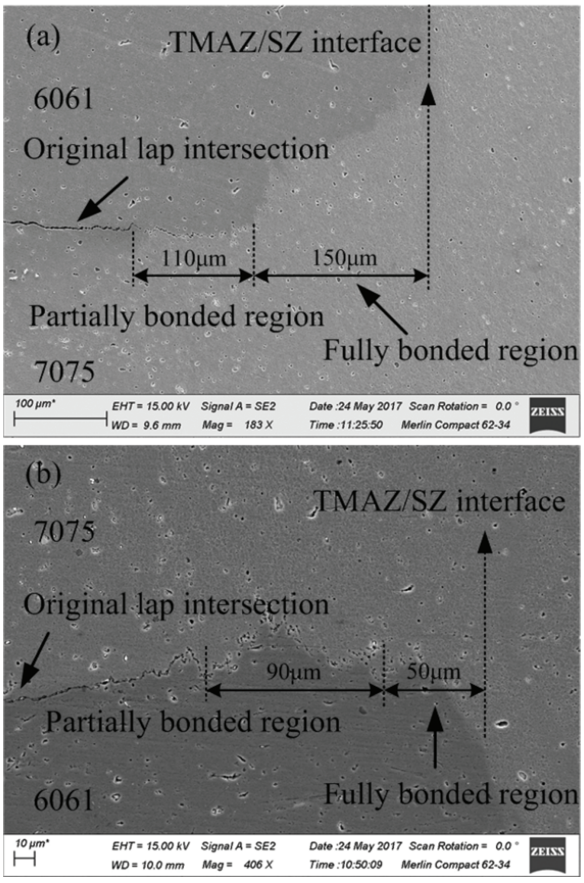

Figure 3: Microstructure of hook region using (a) 6061 and (b) 7075 as the upper sheets.

that using 7075 as the upper sheet. Under this condition, the lap interface was more completely broken (Figure 3 (a)). On the contrary, when using 7075 as the upper sheet, relative weaker material flowability was attained and the smaller bonding width was obtained.

For lap joints, effective lap width (ELW) is an important variable. It clearly reflects the effect of hook on joint quality. In the present work, the ELW on the joint using 6061 as the upper sheet was much bigger than that using 7075 as the upper sheet. In the following section, the microstructure and mechanical properties of the joints using 6061 as the upper sheet were mainly discussed.

Figure 4 shows the cross sections of joints using 6061 as the upper sheets. Similar to the joint using 7075 as the upper sheet, the cross sections presented basin-like morphologies. When using the plunge depth of 3.4 mm, a portion of the 7075 Al stayed at the joint center. The detailed microstructure was discussed in the following part. With increasing the plunge depth, adequate material mixing happened. No un-bonded interface was observed (Figure 4(b–d)). As shown in Figure 4(a), near the hook, a part of 7075 Al showed an upward flowing trend. The height of the upward flowing 7075 Al increased with increasing the plunge depth (Figure 4(b)). As shown in Figure 4, well bonding was

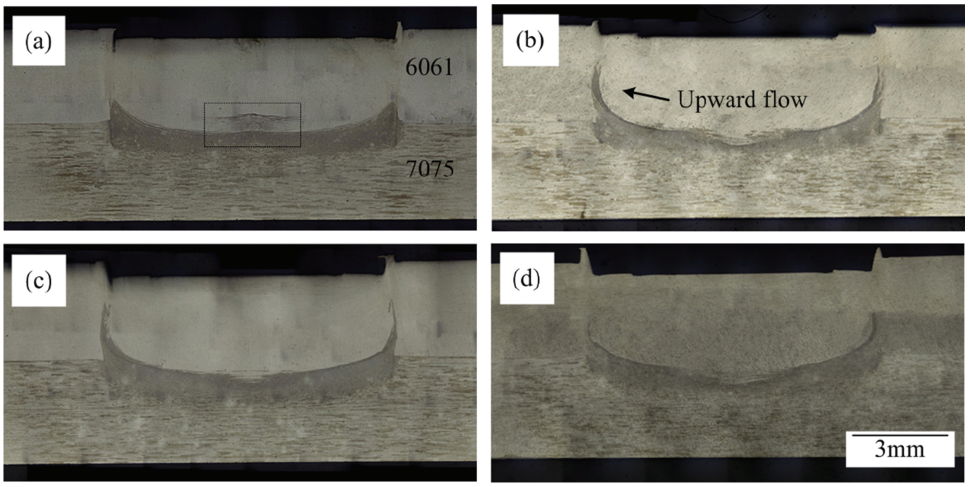

Figure 4: Joint cross sections using (a) 3.4 mm, (b) 3.5 mm, (c) 3.6 mm and (d) 3.7 mm.

formed at the TMAZ/SZ interfaces. So bigger height of the 7075 Al meant more adequate mixing between the BMs.

Figure 5 shows the microstructure of the joint center using 3.4 mm. Lamellar structures were observed at the joint center. The relative light structure was 6061 Al and the relative dark structure was 7075 Al. The bedded structures were formed due to the retraction and rotation of the sleeve. Its formation was very much like that of the onion ring [32]. Figure 5(b) shows the SEM image of the lamellar structures. Figure 5(c–g) shows the element distributions at this region. As Figure 5(c) and 5(d) show, Cu and Zn elements were much obvious. They showed similar morphologies like the lamellar structures in Figure 5 (b). The distributions of Cu and Zn elements showed that rather weak element diffusion happened inside this region. This conclusion proved that FSW was a solid state joining process during which element distribution was rather weak. However, the elements of Fe, Mg and Si showed rather even distribution in this region.

Figure 6 shows the microstructure at lap interface in the joint center using the sleeve plunge depth of 3.8 mm. No lamellar structures were observed. This can be attributed to more adequate material flow behavior when using bigger sleeve plunge depth. No any cracks or voids were observed. Figure 6(b–f) shows the element distribution in this area. Similar to Figure 5, Cu and Zn elements were clearly recognized, while the other three elements presented even distribution. Again, judging from the Cu and Zn element which owned higher content in 7075 Al, it was concluded that diffusion effect in FSW was rather weak.

Shen et al. [13] reported that for 7075 RFSSW joint, defect such as void easily appeared at the maximum sleeve plunge depth region. Figure 7 shows the microstructure of this region using the sleeve plunge depth of 3.8 mm. No defects were observed in Figure 7(a). Due to different etching rates, different regions of the joint were clearly recognized. Commonly, the microstructure of the joint was divided in BM, TMAZ, heat affected zone (HAZ) and SZ. 7075 is one of the typical precipitation-hardening aluminum alloys. The mechanical properties of joint were significantly affected by the secondary phase particles. Figure 7 (b–e) shows the secondary phase particles at different regions. As shown in Figure 7(b), some secondary phases with different sizes were observed at the BM. At the HAZ in Figure 7(c), the secondary phases showed similar morphology like that in Figure 7(b). The TMAZ underwent both mechanical stirring and thermal effect. Thus less secondary phases with smaller sizes were observed (Figure 7(d)). As shown in Figure 7(e), in the SZ, due to the intense mechanical stirring, almost no secondary phases were seen.

Figure 8 shows the lap shear failure loads of joints. As shown in Figure 8, when using the sleeve plunge depth of 3.4 mm, the joint using 6061 as upper owned much higher failure load (10,816 N) than the joint using 7075 as the upper sheet (7,258 N). This can be attributed to the defects in Figure 2 when using 7075 as the upper sheet. For the joints using 6061 Al as the upper sheet, with increasing the sleeve plunge depth, lap shear failure load firstly increased and then decreased. The maximum failure load of 12,892 N was attained when using the sleeve plunge depth of 3.6 mm.

Figure 9(a) shows the fracture position of the joint. The joint failed at the 7075 Al which flowed upwards. Therefore, there existed one optimum upward flow height of the 7075 Al. When using small plunge depth, the material mixing between the two BMs was weak. With increasing the plunge depth, material mixing became

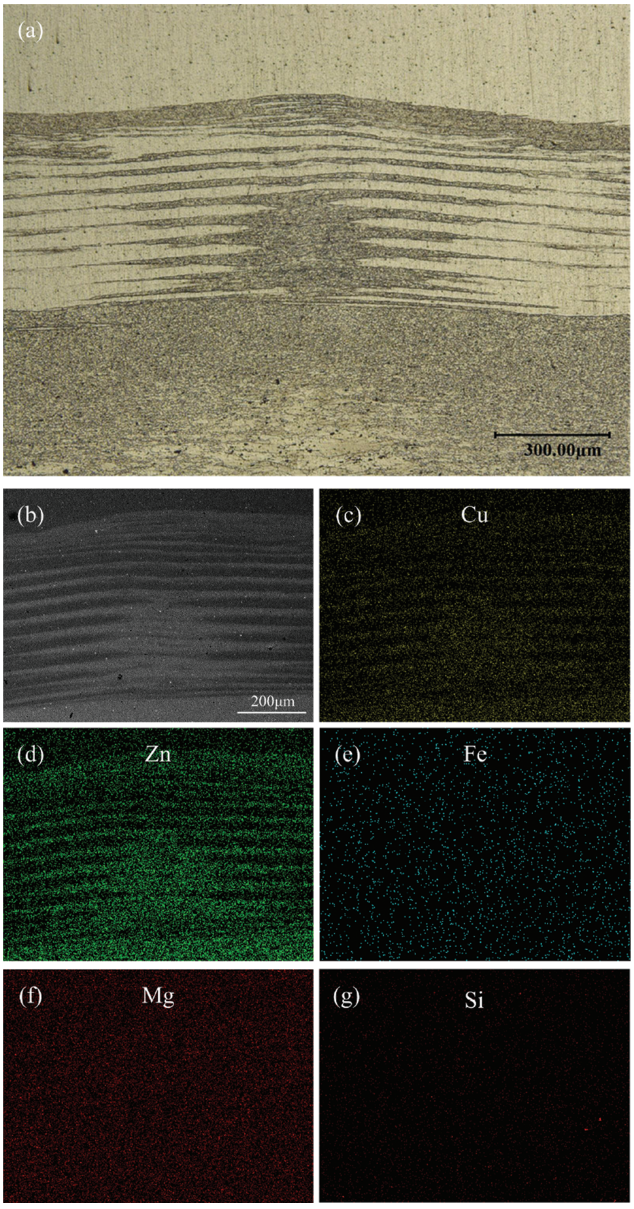

Figure 5: Microstructure of the joint using 3.4 mm: (a) joint center, (b) SEM image, (c) Cu, (d) Zn, (e) Fe, (f) Mg and (g) Si.

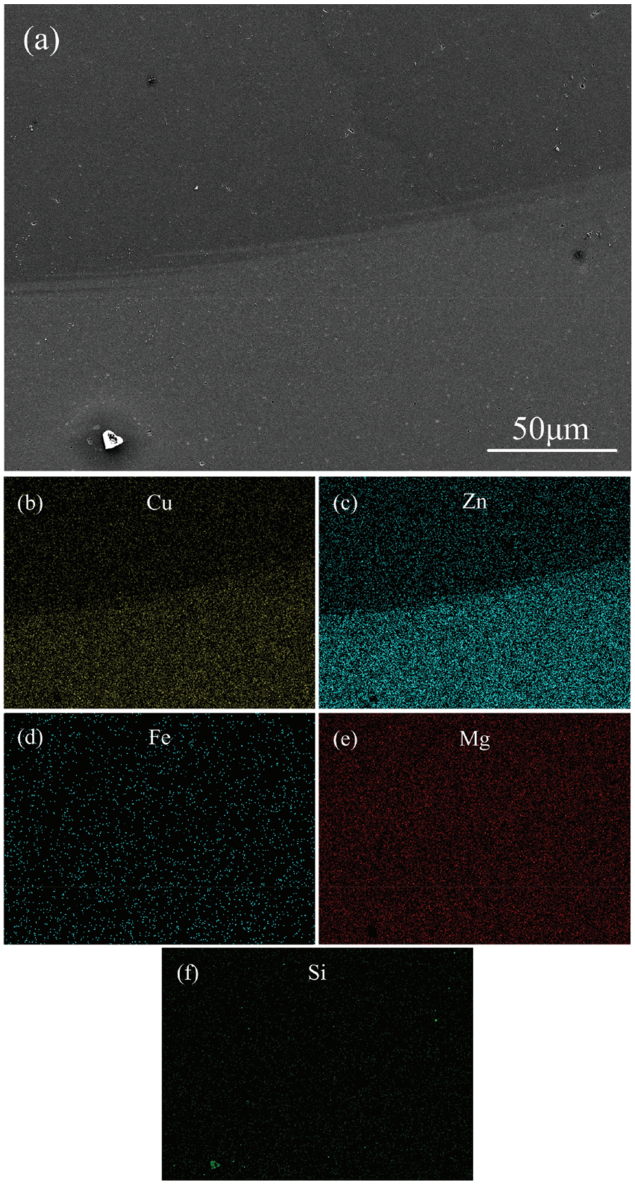

Figure 6: Microstructure of the joint using 3.8 mm: (a) SEM image of joint center, (b) Cu, (c) Zn, (d) Fe, (e) Mg and (f) Si.

better and therefore lap shear failure load increased. With further increasing the sleeve plunge depth, more heat input may soften the upward flow 7075 Al. Therefore, joint strength showed a decrease.

Conclusions

1) Defects such as void, unbonded interface and incomplete refilling are observed when using 7075 Al as the upper sheet. No defects are observed when using 6061 Al as the upper sheet.
2) With increasing the sleeve plunge depth, better material mixing happens between the upper and lower sheets.
3) Joint using 6061 as the upper sheet shows much high lap shear failure load than joint using 7075 as the upper sheet.
4) With increasing the sleeve plunge depth, the lap shear failure load of joint firstly increases and then decreases. The maximum failure load of 12,892 N was obtained when using the sleeve plunge depth of 3.6 mm.

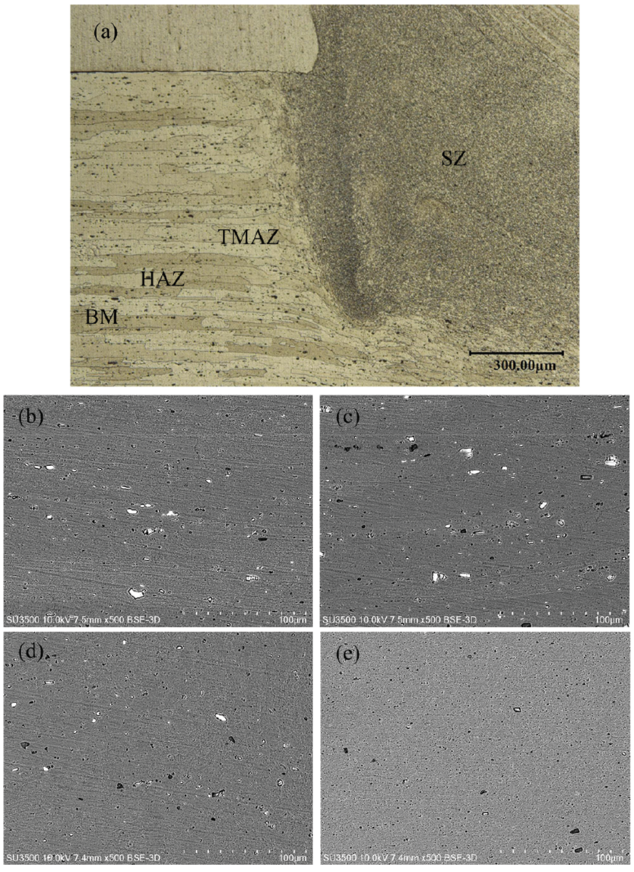

Figure 7: Secondary phases near the maximum plunge depth region: (a) the general view, (b) BM, (c) HAZ, (d) TMAZ and (e) SZ.

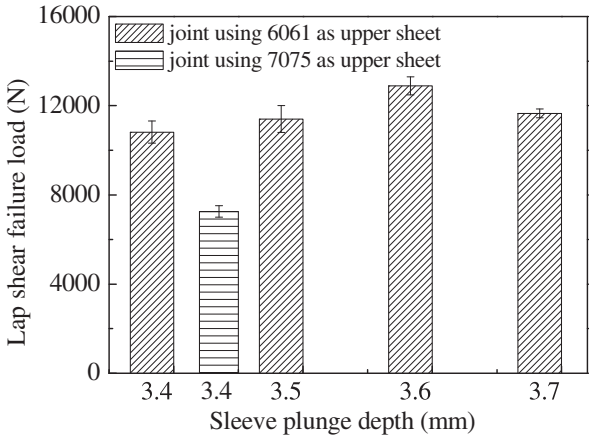

Figure 8: Lap shear failure loads of the joints.

Acknowledgements: This work is supported by the China Postdoctoral Science Foundation (No.2016M590821), the Guangdong Key Laboratory of Enterprise Advanced Welding Technology for Ships (2017B030302010).

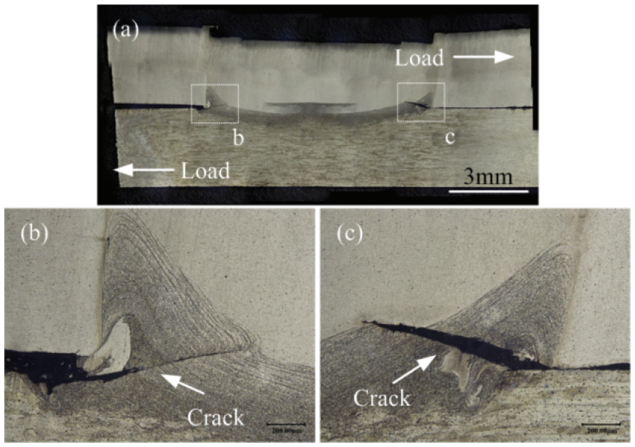

Figure 9: Fracture position of the joint: (a) general view, (b) and (c) magnified views of the fracture positions.

References

[1] Y. Yue, Q. Wen, S. Ji, L. Ma and Z. Lv, High. Temp. Mater. Process, 2016 10.1515/htmp-2015-0178.
[2] Y. Huang, X. Meng, Y. Zhang, J. Cao and J. Feng, J. Mater. Process. Technol., 250 (2017) 313–319.
[3] Y. Song, X. Yang, L. Cui, X. Hou, Z. Shen and Y. Xu, Mate. Des., 55 (2014) 9–18.
[4] Z. Yan, X. Liu and H. Fang, J. Mater. Sci. Technol., 32 (2016) 1378–1385.
[5] M.M.Z. Ahmed, B.P. Wynne, W.M. Rainforth and P.L. Threadgill, Scr. Mater., 64 (2011) 45–48.
[6] H.S. Fujii, Y.F. Sun, I.K. Kato and K. Nakata, Mater. Sci. Eng. A, 527 (2010) 3386–3391.
[7] G. Buffa, L. Fratini, M. Schneider and M. Merklein, J. Mater. Process. Technol., 213 (2013) 2312–2322.
[8] S. Ji, Z. Li, L. Zhang and Y. Wang, Mater. Lett., 188 (2017) 21–24.
[9] P. Xue, B.B. Wang, F.F. Chen, W.G. Wang, B.L. Xiao and Z.Y. Ma, Mater. Charact., 121 (2016) 187–194.
[10] Y.F. Sun, H. Fujii, N. Takaki and Y. Okitsu, Mater. Des., 37 (2012) 384–392.
[11] M. Avettand-Fènoël and A. Simar, Mater. Charact., 120 (2016) 1–17.
[12] J.F. Guo, H.C. Chen, C.N. Sun, G. Bi, Z. Sun and J. Wei, Mater. Des., 56 (2014) 185–192.
[13] Y.Q. Zhao, H.J. Liu, Z. Lin, S.X. Chen and J.C. Hou, Sci. Technol. Weld. Join., 19 (2014) 617–622.
[14] Y.Q. Zhao, H.J. Liu, S.X. Chen, Z. Liu and J.C. Hou, Mater. Des., 62 (2014) 40–46.
[15] Z.K. Shen, X.Q. Yang, Z.H. Zhang, L. Cui and T.L. Li, Mater. Des., 44 (2012) 476–486.
[16] Z. Li, S. Ji, Y. Ma, P. Chai, Y. Yue and S. Gao, Int. J. Adv. Manuf. Technol., 86 (2016) 1925–1932.
[17] U.F.H. Suhuddin, V. Fischer and J.F. Dos Santos, Scripta. Mater., 68 (2013) 87–90.
[18] U. Suhuddin, V. Fischer, F. Kroeff and J.F. Dos Santos, Mater. Sci. Eng. A, 590 (2014) 384–389.

[19] L.C. Campanelli, U.F.H. Suhuddin, A.S. Antonialli, J.F. Dos Santos, N.G. de Alcantara and C. Bolfarini, J. Mater. Process. Technol., 213 (2013) 515–521.
[20] M.A.D. Tier, T.S. Rosendo, J.F. Dos Santos, N. Huber, J.A. Mazzaferro, C.P. Mazzaferro and T.R. Strohaecker, J. Mater. Process. Tech., 213 (2013) 997–1005.
[21] C. Gao, R. Gao and Y. Ma, Mater. Des., 83 (2013) 719–727.
[22] T. Rosendo, B. Parra, M.A.D. Tier, A.A.M. Da Silva, J.F. Dos Santos and T.R. Strohaecker, Mater. Des., 32 (2011) 1094–1100.
[23] H. Dong, S. Chen, Y. Song, X. Guo, X. Zhang and Z. Sun, Mater. Des., 94 (2016) 457–466.
[24] A.H. Plaine, A.R. Gonzalez, U.F.H. Suhuddin, J.F. Dos Santos and N.G. Alcantara, Mater. Des., 83 (2015) 36–41.
[25] P.H.F. Oliveira, S.T. Amancio-Filho, J.F. Dos Santos and E. Hage, Mater. Lett., 64 (2010) 2098–2101.
[26] A.H. Plaine, U.F.H. Suhuddin, N.G. Alcântara and J.F. Dos Santos, Int. J. Fatigue., 91 (2016) 149–157.
[27] J.Y. Cao, M. Wang, L. Kong and L.J. Guo, J. Mater. Process. Technol., 230 (2016) 254–262.
[28] J.Y. Cao, M. Wang, L. Kong, H.X. Zhao and P. Chai, Mater. Charact., 128 (2017) 54–62.
[29] Z. Li, S. Gao, S. Ji, Y. Yue and P. Chai, J. Mater Eng. Perform., 25 (2016) 1673–1682.
[30] Z. Li, Z. Xu, L. Zhang and Z. Yan, Materi. Sci. Technol., 33 (2017) 1626–1634.
[31] Z. Xu, Z. Li, S. Ji and L. Zhang, J. Mater. Sci. Technol., 2017 https://doi.org/10.1016/j.jmst.2017.02.011.
[32] L. Wan, Y. Huang, W. Guo, S. Lv and J. Feng, J. Mater. Sci. Technol., 30 (2014) 1243–1250.